PHOTOACOUSTIC AND ULTROSOUND DUAL-MODALITY ENDOSCOPIC IMAGING BASED ON ALN PMUT ARRAY

Junxiang Cai[1,2,3], Yiyun Wang[1,2,3*], Liang Lou[4], Songsong Zhang[4], Yuandong (Alex) Gu[4], Fei Gao[1,2,3], Tao Wu[1,2,3]*

[1]School of Information Science and Technology, ShanghaiTech University, China
[2]Shanghai Institute of Microsystem and Information Technology, Chinese Academy of Sciences, China
[3]University of Chinese Academy of Sciences, China
[4]Shanghai Industrial μTechnology Research Institute, China

2022 IEEE 35th International Conference on Micro Electro Mechanical Systems Conference (MEMS) | 978-1-6654-0911-7/22/$31.00 ©2022 IEEE | DOI: 10.1109/MEMS51670.2022.9699511

ABSTRACT

This article reports an aluminum nitride(AlN) piezoelectric micromachined ultrasound transducer (PMUT) array enabling dual imaging modality of photoacoustic (PA) and ultrasound (US) endoscopy. AlN is a kind of non-toxic material, making it suitable for biomedical, especially implantable applications. In clinical endoscopic imaging, pulse-echo US signal can distinguish soft tissues' mechanical properties easily, while PA signal is more sensitive to tissues' optical absorption property. Both US and PA signals can be received by fabricated AlN PMUT array. This dual-modal endoscopic imaging provides doctors both structural and functional information for accurate diagnostics. Moreover, the miniature size of MEMS PMUT is highly potential to enable intravascular imaging within 1 mm diameter in the future.

KEYWORDS

Photoacoustic imaging, ultrasound imaging, AlN PMUT array, dual-modality endoscope.

INTRODUCTION

As a new rapidly growing tool, photoacoustic imaging (PAI) studies biological tissues with the configuration of laser excitation and ultrasonic reception [1–3]. Based on the optical absorption contrast, such as hemoglobin and melanin, PAI mainly provides functional information, utilizing either endogenous or exogenous contrast agents [4, 5]. It complements the ultrasound imaging (USI) by revealing morphological information [5]. Hybrid imaging modalities, like the dual modality of photoacoustic and ultrasound imaging, offer comprehensive information that are closer to clinical needs. Sharing the same ultrasonic receiving system, the photoacoustic and ultrasound methods are studied widely as dual-modality imaging system [6]. The comprehensive information provided by the integrated system may enhance diagnostic accuracy, compared with conventional methods.

For practical clinical application scenario, the imaging system trends to be compact, portable, and integrated. However, the bulky size and optical opaque of the conventional piezoelectric transducers bring challenges to the systems' integration [7]. Recently, researchers introduced micromachined ultrasonic transducers, such as piezoelectric micromachined ultrasonic transducer (PMUT), into photoacoustic sensing and imaging.

PAI can achieve high spatial resolution, larger imaging depth and rich optical contrast with smaller, faster and less expensive system. PAI is efficient for the early cancer detection of breast, prostate, pancreatic and colorectal cancer [8, 9]. Due to the strong attenuation of the excitation laser in human tissues, the image depth is still limited to <5 cm, which makes it hard to diagnose deep inside human body, like gut and deep blood vessels. As a result, endoscopy imaging with miniature technology is highly required. Conventional bulk piezoelectric transducer is limited by its size and fabrication in the usage of endoscopy [10], while capacitive micromachined ultrasound transducer (CMUT) and PMUT based on MEMS technology can make tiny endoscope for PAI and USI. CMUT has a high sensitivity and wide bandwidth, but it requires high bias voltage ,which can cause safety risk in biomedical in vivo imaging application [11]. PMUTs are usually divided into two types according to the working mode: thickness extension mode (TEM) and flexural vibration mode (FVM). Different TEM PMUTs have been fabricated and applied in PAI based on PZT [12–14], PVDF [15, 16], PMN-PT, $LiNbO_3$[17]. TEM PMUTs based on single-crystal PMN-PT and ceramic PZT have high frequency and high sensitivity due to the superior piezoelectric constants of PZT and PMN-PT. However, TEM PMUTs have drawbacks of small bandwidth and low imaging speed in endoscopic PAI. Compared to the TEM PMUTs, FVM PMUTs have lower acoustic impedance and larger bandwidth. In addition, the FVM PMUT is easier to manufacture and form arrays for higher sensitivity and more functionality. Typically, ZnO, PZT, and AlN are mostly used to fabricate FVM PMUT [11]. Compared with ZnO and PZT, AlN has better chemical and thermal stability and biosafety, and it is also compatible with complementary metal-oxide semiconductor (CMOS) fabrication process [18, 19], which makes the CMOS-MEMS monolithic transducer chip possible. FVM PMUT based ALN have similar advantages including bandwidth, biosafety, thermal stability and convenient integration in the application of ultrasound imaging.

Endoscopic photoacoustic imaging [11] and ultrasound imaging [20] based on PMUT have been separately reported, but the combination of the two technologies hasn't been extensively studied. This article reports an AlN PMUT array enabling dual imaging modality of photoacoustic and ultrasound endoscopy.

PMUT FABRICATION AND ANALYSIS

The presented dual-modality endoscopic imaging is based on AlN PMUT. Fig. 1 shows a circular PMUT membrane design. The PMUT device is fabricated on SOI (Silicon-On-Insulator) wafer, and AlN thin film is its piezoelectric layer. Molybdenum (Mo) layers are used as the top and bottom electrodes to collect the charge of AlN

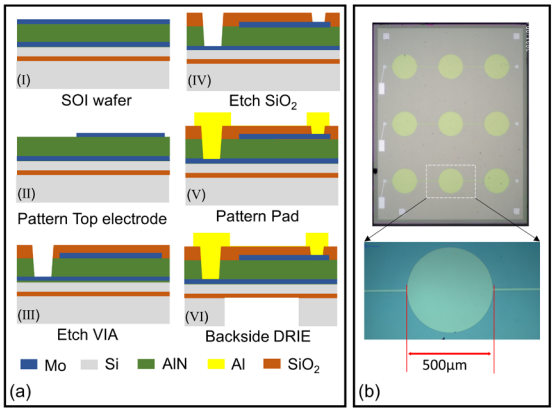

Figure 1: Fabrication of PMUT array. (a) Process flow. (b) Optical image of PMUT device.

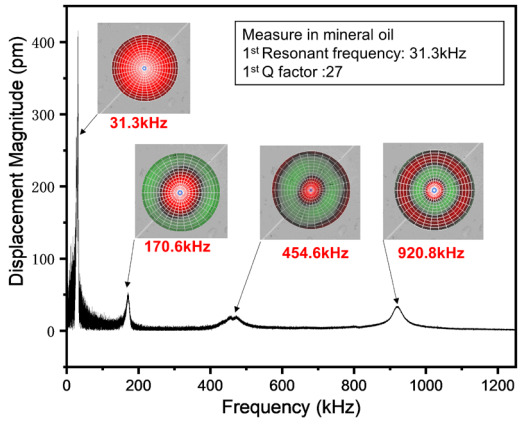

Figure 2 The LDV measurement of the PMUT array in mineral oil.

piezoelectric layer. On the other hand, the Mo electrodes can drive the AlN piezoelectric layer by applying voltage. Top silica layer is used to protect thin film. Through two-step etching (III-IV), material aluminum can connect the bottom electrode and the top electrode to the surface for wire bounding (V). Finally a backside DRIE process (VI) creates cavities, which defines the effective flexural membrane diameter of the PMUT cell. The optical picture of the PMUT array is shown in Fig. 1(b). The PMUT array contains three individual channels, and etch channel contains three same cells with top electrodes connected together. The cell's diameter is about 500 μm.

PMUT produced through the process flow shown in Fig. 1(a) usually works in FVM, which is primarily caused by the d_{31} mode excitation [21, 22]. FVM PMUT has a large capacitance and low electrical impedance, making it more robust against parasitic effects and better matched to readout electronics [23].

Resonance frequency is one of the most important parameters of PMUT for PAI and USI applications. For a circular PMUT membrane design, the resonance frequency is mainly determined by the radius of circular membrane of PMUT. PMUT's material and membrane thickness can also affect resonance frequency. But in fabrication, these parameters are usually not changed in once fabrication. The fundamental resonance frequency in air can be defined by the following formula [24]:

$$f_{air} = \frac{3.2^2}{2\pi a^2}\sqrt{\frac{D}{\rho}} \qquad (1)$$

where a is radius, D is equivalent flexural rigidity of thin flim, and ρ is the average area mass density of the membrane.

It's common for a biological endoscopy imaging working in liquid environment. Liquid can be a considerable coupling medium for better acoustic impedance matching. However, PMUT's resonance frequency will drop in liquid, which can be expressed by following equation (2):

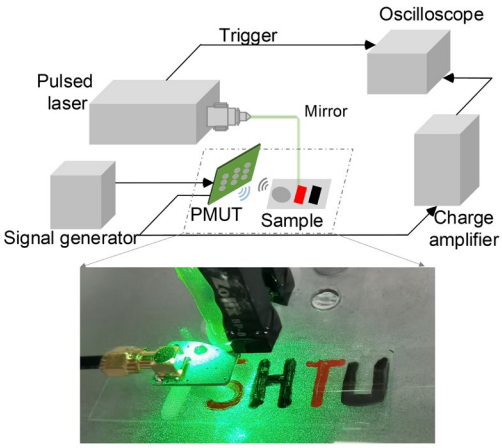

Figure 3: Set up of photoacoustic and ultrasound dual modality imaging.

$$f_{liquid} = \frac{f_{air}}{\sqrt{1+\frac{M_a}{M_m}}} \qquad (2)$$

where f_{air} is the fundamental resonance frequency in air, M_a is the added mass of liquid, and the M_m is the mass of membrane. The M_a can be calculated by [25]:

$$M_a = 0.67 \cdot \pi \cdot \rho_{liquid} \cdot a^3 \qquad (3)$$

Fig. 2 shows the frequency response and vibration modes of PMUT measured by LDV in mineral oil. The frequency and Q factor are 31.3 kHz and 27. The resonant frequency and mode shape of the second to fourth order are also shown. The LDV measurement data indicate significant drop of resonance frequency and Q factor when PMUT is working in liquid environment compared with the similar device working in air [21]. The decrease in frequency is not conducive to the lateral resolution, but the increased bandwidth is in favor of the axial resolution improvement.

DUAL-MODALITY ENDOSCOUPY

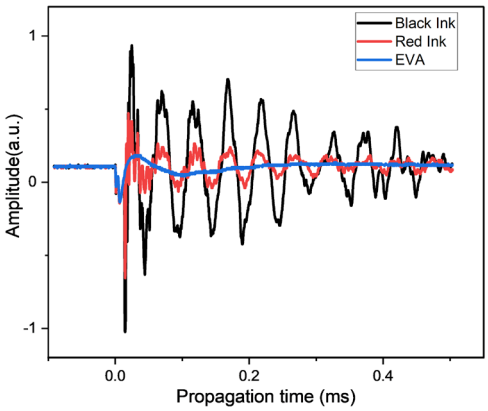

Figure 4. PA signals of different components on the sample. The signal's amplitude of components with black ink is larger than that with red ink. EVA component's signal amplitude is the weakest.

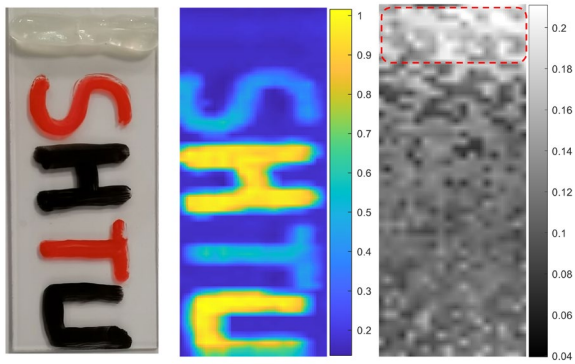

Figure 5. Results of dual-modality imaging. (a). Optical image of the sample. (b) Sample's photoacoustic imaging. (c) Ultrasound image of the sample.

SYSTEMS

The setup of dual-modality imaging is shown in Fig. 3, which composes of pulsed laser generator, fiber, signal generator, charge amplifier, oscilloscope, PMUT device and testing sample. The magnification of the charge amplifier is about 1V/10pC. The fabricated PMUT shown in Fig. 1(b) is served as the acoustic sensor for both PA and US signals, and the transmitter for USI. The PMUT is connected to the PCB as shown in Figure 3, with the surface facing the sample. The laser is irradiated on the sample through the hole on the PCB board.

In PAI, the pulse laser light emitted by the laser generator irradiates the sample through the fiber. Due to the effect of rapid thermal expansion, the irradiated area emits ultrasonic waves. PMUT senses the ultrasound wave and converts the ultrasound wave into electric signal. In USI, a signal generator sends a short electrical signal to the PMUT to transmit ultrasonic waves, and then the same PMUT will sense phantom's structural information from reflection wave. The charge amplifier amplifies the output signal of PMUT, then the amplified signal passes through a high-pass filter to eliminate low-frequency interference. Then, the oscilloscope collects and displays these signals. Through the communication between the oscilloscope and the computer, MATLAB gets the data and analyze them. The two imaging modalities can be achieved in one scan with the proper control of software and hardware.

IMAGING RESULT AND ANALYSIS

Two preliminary experiments are performed for the demonstration of the photoacoustic and ultrasound endoscopy that is based on the AlN PMUT array design. We first fabricate the sample, which is a glass slide with a strip of ethylene vinyl acetate (EVA), red ink letter 'S' and 'T', and black ink letter 'H' and 'U'. Then, we verify the feasibility of photoacoustic sensing with the certain designed PMUT array and a 532 nm pulsed laser. Lastly, by applying two-dimensional scanning, ultrasound and photoacoustic images of the sample are obtained based on the aforementioned PMUT array design.

The time-domain waveforms of the three generated PA signals from the sample are shown in Fig. 4, respectively. All signals are passed through a 10kHz high-pass filter to avoid low-frequency noise. The main frequency of these three signals is around 30kHz, which corresponds to the fundamental resonance frequency of PMUT. The amplitude of the EVA's signal is weak, which indicates the neglectable optical absorption. The components with inks have prominent peak signals. Since the designed PMUT is a narrow-band transducer, the PA signals show oscillation. According to the different optical absorptance, the maximum peak's amplitude of black-ink components' signals is larger than that of red-ink components' signals, which is also demonstrated in Fig. 4.

For demonstration of dual-modality imaging with the PMUT array integrated device, a bionic board is used as imaging target. Shown in Fig. 5(a), the phantom has a red ink "ST" and a black ink "HU" to simulate biological tissues with different light absorptance, and the top part is ethylene viny acetate (EVA) to simulate the plaque tissue with weak optical absorption that is not able to be detected by PA imaging. This phantom was scanned in a 2 cm×5.5 cm region with a step size of 1 mm. Fig. 5(b) presents the PA image with clear "SHTU", where "ST" is lighter than "HU" indicating that tissues with different light absorption can be distinguished. The EVA part that cannot be imaged in PA image, which however can be detected by ultrasound imaging modality (Fig. 5(c)). From the photoacoustic imaging result, the letters are visible while EVA's shape is vague. The black letters generate stronger PA signals than the red letters. It shows the system's capability of discriminating functional information based on optical absorption in the PA mode. On the other hand, the system images the morphological information in the US mode. By combining PA and US imaging results, the phantom's structural and functional information is completely restored. This combination can make the endoscope more efficient for medical applications.

CONCLUSION

A FVM AlN PMUT array are fabricated for the application of both PAI and USI. The LDV measures the

resonance frequency and vibration shape of PMUT. Dual modality imaging system realizes the simultaneous acquisition of photoacoustic signal and ultrasonic signal. The PMUT array are tiny enough to be integrated into intestinal or vascular endoscopes. Compared with single PAI and signal USI, the dual modality endoscopy imaging can acquire more complete information.

ACKNOWLEDGEMENTS

The authors appreciate the PMUT fabrication support from SITRI and ShanghaiTech Quantum Device Lab (SQDL), Natural Science Foundation of Shanghai (19ZR1477000), Pujiang Talent Program（19PJ1432300）and National Natural Science Foundation of China (61874073).

REFERENCES

[1] C. Lee, J. Y. Kim, C. Kim, "Recent progress on photoacoustic imaging enhanced with microelectromechanical systems (MEMS) technologies," *Micromachines*, vol. 9, no. 11, pp. 25–28, 2018.

[2] L. V. Wang, "Tutorial on photoacoustic microscopy and computed tomography," *IEEE J. Sel. Top. Quantum Electron.*, vol. 14, no. 1, pp. 171–179, 2008.

[3] D. Biqin, C. Sun, H. F. Zhang, "Optical Detection of Ultrasound in Photoacoustic Imaging," *IEEE Trans. Biomed. Eng.*, vol. 64, no. 1, pp. 4–15, 2017.

[4] A. B. E. Attia, G. Balasundaram, M. Moothanchery, U. S. Dinish, R. Bi, V. Ntziachristos, M. Olivo, "A review of clinical photoacoustic imaging: Current and future trends," *Photoacoustics*, vol. 16, no. November, p. 100144, 2019.

[5] T. Guo, K. Xiong, Z. Zhang, L. Li, S. Yang, "In vivo anatomical imaging of colorectum by tens-of-micron-resolved photoacoustic/ultrasonic endoscope," *Appl. Phys. Lett.*, vol. 118, no. 15, 2021.

[6] J. Kim, S. Park, Y. Jung, S. Chang, J. Park, Y. Zhang, J. F. Lovell, C. Kim, "Programmable Real-time Clinical Photoacoustic and Ultrasound Imaging System," *Sci. Rep.*, vol. 6, no. October, pp. 1–11, 2016.

[7] D. Biqin, C. Sun, H. F. Zhang, "Optical Detection of Ultrasound in Photoacoustic Imaging," *IEEE Trans. Biomed. Eng.*, vol. 64, no. 1, pp. 4–15, 2017.

[8] M. Mehrmohammadi, S. Joon Yoon, D. Yeager, S. Y Emelianov, "Photoacoustic imaging for cancer detection and staging," *Curr. Mol. Imaging Discontin.*, vol. 2, no. 1, pp. 89–105, 2013.

[9] X. Leng, W. Chapman, B. Rao, S. Nandy, R. Chen, R. Rais, I. Gonzalez, Q. Zhou, D. Chatterjee, M. Mutch, "Feasibility of co-registered ultrasound and acoustic-resolution photoacoustic imaging of human colorectal cancer," *Biomed. Opt. Express*, vol. 9, no. 11, pp. 5159–5172, 2018.

[10] K. K. Shung, J. M. Cannata, Q. F. Zhou, "Piezoelectric materials for high frequency medical imaging applications: A review," *J. Electroceramics*, vol. 19, no. 1, pp. 141–147, 2007.

[11] H. Wang, Y. Ma, H. Yang, H. Jiang, Y. Ding, H. Xie, *Mems ultrasound transducers for endoscopic photoacoustic imaging applications*, vol. 11, no. 10. 2020.

[12] Y. Li, R. Lin, C. Liu, J. Chen, H. Liu, R. Zheng, X. Gong, L. Song, "In vivo photoacoustic/ultrasonic dual-modality endoscopy with a miniaturized full field-of-view catheter," *J. Biophotonics*, vol. 11, no. 10, p. e201800034, 2018.

[13] Y. Li, X. Gong, C. Liu, R. Lin, W. Hau, X. Bai, L. Song, "High-speed intravascular spectroscopic photoacoustic imaging at 1000 A-lines per second with a 0.9-mm diameter catheter," *J. Biomed. Opt.*, vol. 20, no. 6, p. 065006, 2015.

[14] X. Dai, L. Xi, C. Duan, H. Yang, H. Xie, H. Jiang, "Miniature probe integrating optical-resolution photoacoustic microscopy, optical coherence tomography, and ultrasound imaging: proof-of-concept," *Opt. Lett.*, vol. 40, no. 12, pp. 2921–2924, 2015.

[15] J. Xiao, Y. Li, W. Jin, K. Peng, Z. Zhu, B. Wang, "Photoacoustic endoscopy with hollow structured lens-focused polyvinylidine fluoride transducer," *Appl. Opt.*, vol. 55, no. 9, pp. 2301–2305, 2016.

[16] N. Liu, S. Yang, D. Xing, "Photoacoustic and hyperspectral dual-modality endoscope," *Opt. Lett.*, vol. 43, no. 1, pp. 138–141, 2018.

[17] J.-M. Yang, C. Favazza, R. Chen, J. Yao, X. Cai, K. Maslov, Q. Zhou, K. K. Shung, L. V. Wang, "Simultaneous functional photoacoustic and ultrasonic endoscopy of internal organs in vivo," *Nat. Med.*, vol. 18, no. 8, pp. 1297–1302, 2012.

[18] Y. Lu, A. Heidari, S. Shelton, A. Guedes, D. A. Horsley, "High frequency piezoelectric micromachined ultrasonic transducer array for intravascular ultrasound imaging," in *2014 IEEE 27th International Conference on Micro Electro Mechanical Systems (MEMS)*, 2014, pp. 745–748.

[19] Z. Luo, S. Shao, T. Wu, "Characterization of AlN and AlScN film ICP etching for micro/nano fabrication," *Microelectron. Eng.*, vol. 242, p. 111530, 2021.

[20] J. Jung, W. Lee, W. Kang, E. Shin, J. Ryu, H. Choi, "Review of piezoelectric micromachined ultrasonic transducers and their applications," *J. Micromechanics Microengineering*, vol. 27, no. 11, p. 113001, 2017.

[21] J. Cai, K. Liu, L. Lou, S. Zhang, Y. A. Gu, T. Wu, "Increasing Ranging Accuracy of Aluminum Nitride Pmuts by Circuit Coupling," in *2021 IEEE 34th International Conference on Micro Electro Mechanical Systems (MEMS)*, Jan. 2021, pp. 740–743.

[22] Z. Luo, S. Shao, T. Wu, "AlN Contour Mode Resonators with Half Circle Shaped Reflectors," in *2021 IEEE 16th International Conference on Nano/Micro Engineered and Molecular Systems (NEMS)*, 2021, pp. 1255–1258.

[23] Y. Qiu, J. V. Gigliotti, M. Wallace, F. Griggio, C. E. M. Demore, S. Cochran, S. Trolier-McKinstry, "Piezoelectric Micromachined Ultrasound Transducer (PMUT) Arrays for Integrated Sensing, Actuation and Imaging," *Sensors*, vol. 15, no. 4, Art. no. 4, Apr. 2015.

[24] Y. Lu, D. A. Horsley, "Modeling, Fabrication, and Characterization of Piezoelectric Micromachined Ultrasonic Transducer Arrays Based on Cavity SOI Wafers," *J. Microelectromechanical Syst.*, vol. 24, no. 4, pp. 1142–1149, Aug. 2015.

[25] R. D. Blevins, R. Plunkett, "Formulas for Natural Frequency and Mode Shape," *J. Appl. Mech.*, vol. 47, p. 461, Jan. 1980.

CONTACT

*Junxiang Cai; caijx1@shanghaitech.edu.cn;
*Yiyun Wang; wangyy@shanghaitech.edu.cn;
First two authors contribute equally.